J Mol Model (2012) 18:3439–3444
DOI 10.1007/s00894-011-1305-z

SHORT COMMENT

# $h\beta_2R$–$G\alpha_s$ complex: prediction versus crystal structure—how valuable are predictions based on molecular modeling studies?

**Andrea Straßer · Hans-Joachim Wittmann**

Received: 18 August 2011 / Accepted: 7 November 2011 / Published online: 6 December 2011


**Abstract** In 2010, we predicted two models for the $h\beta_2R$–$G\alpha_s$ complex by combining the technique of homology modeling with a potential energy surface scan, since a complete crystal structure of the $h\beta_2R$–$G\alpha_s$ complex was not available. The crystal structure of opsin co-crystallized with part of the C-terminus of Gα (3DQB) was used as a template to model the $h\beta_2R$, whereas the crystal structure of Gα (1AZT) was used as a template to model $G\alpha_s$. Utilizing a potential energy surface scan between $h\beta_2R$ and $G\alpha_s$, a six-dimensional potential energy surface was obtained. Two significant minimum regions were located on this surface, and each was associated with a distinct $h\beta_2R$–$G\alpha_s$ complex, namely model I and model II [Straßer A, Wittmann H-J (2010) J Mol Model 16:1307–1318]. The crystal structure of the $h\beta_2R$–$G\alpha_s\beta\gamma$ complex has recently been published. Thus, the aim of the current study was, on the one hand, to compare our predicted structures with the true crystal structure, and on the other to discuss the question: how valuable are predictions based on molecular modeling studies?

**Keywords** GPCR–Gα complex · Prediction · Molecular modeling · Energy surface scan · Crystal structure

Andrea Straßer and Hans-Joachim Wittmann both contributed equally to this work.

A. Straßer (✉)
Department of Pharmaceutical and Medicinal Chemistry II,
Faculty of Chemistry and Pharmacy, University of Regensburg,
Universitätsstraße 31,
93040 Regensburg, Germany
e-mail: andrea.strasser@chemie.uni-regensburg.de

H.-J. Wittmann
Faculty of Chemistry and Pharmacy, University of Regensburg,
Universitätsstraße 31,
93040 Regensburg, Germany

## Introduction

G protein-coupled receptors (GPCRs) consist of seven transmembrane (TM) domains that are located in a lipid bilayer. The TM domains are connected by intra- and extracellular loops. In the intracellular part, the GPCRs couple to heterotrimeric G proteins, which consist of Gα, Gβ, and Gγ subunits [1, 2]. The binding of an agonist to a GPCR results in a switch from an inactive into an active conformation. In its active conformation, the GPCR is able to interact with the G protein [3, 4].

Crystal structures of GPCRs such as the adrenergic $\beta_1$, adrenergic $\beta_2$, and adenosine $A_{2A}$ as well as the crystal structures of $G\alpha\beta\gamma$ units had been published as of 2010 [5–10], and the crystal structure of opsin co-crystallized with 11 amino acids of the C-terminus of the Gα subunit was published in 2008 [11]. However, as of 2010, the crystal structure of the complete GPCR–Gα complex was not yet available. Since detailed knowledge of the interaction between GPCR and G protein is needed to understand the functionality of GPCR at the molecular level, we used molecular modeling techniques to predict the structure of a complex between active $h\beta_2R$ and $G\alpha_s$ [12]. Thus, based on the crystal structure of opsin (3DQB) [11], an active state model of $h\beta_2R$, and the crystal structure of $G\alpha_s$ (1AZT) [13], a model of $G\alpha_s$ was generated, as previously described [12]. Using both homology models in combination with a potential energy surface scan, two active $h\beta_2R$–$G\alpha_s$ models (models I and II, Fig. 1) were predicted [12]. Recently, the crystal structure of the whole $h\beta_2R$–$G\alpha\beta\gamma$ complex (3SN6) was published [14]. Thus, in this work, in order to determine the value of predictions based on molecular modeling studies, we compare our predicted models with the experimentally determined crystal structure.

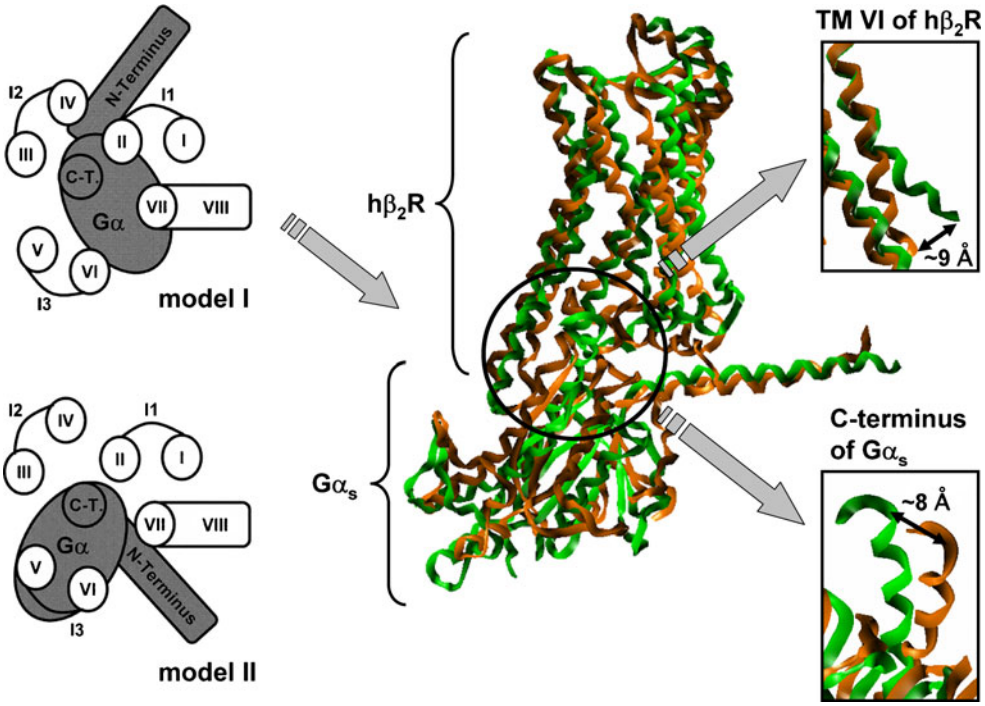


**Fig. 1** Comparison of predicted model I with the corresponding parts of the crystal structure 3SN6. Model I and model II for the $h\beta_2R$–$G\alpha_s$ complex (obtained in previous modeling studies [12]). Alignment of model I (*orange*) and the corresponding part of the crystal structure 3SN6 (*green*). The largest differences were found in relation to TM VI of $h\beta_2R$ and the C-terminus of $G\alpha_s$

## Results and discussion

### Comparison of the predicted model with the crystal structure

In our modeling studies, a model of $h\beta_2R$ obtained using the crystal structure of opsin (3DQB) [11] as a template was generated by homology modeling [12]. This model incorporated the E2 loop from the crystal structure of $h\beta_2R$ (2RH1, [6–8]). Alignment of the backbones of the modeled $h\beta_2R$ (model I, Fig. 1) [12] and $h\beta_2R$ from the crystal structure (3SN6) results in an RMSD of about 2.4 Å (Fig. 1). The largest differences are observed in the intracellular part of TM VI (Fig. 1). Compared to our homology model, TM VI of the crystal structure 3SN6 exhibits greater outward movement (~8 Å).

The crystal structure (3SN6) exhibited an unexpected orientation of the $G\alpha_s$AH domain [14]. Thus, when calculating the RMSD between our $G\alpha_s$ homology model and the $G\alpha_s$ of the crystal structure (3SN6), we did not include the corresponding amino acids (K301–V415 [12]). Alignment of the backbones of both structures revealed an RMSD of 3.5 Å (Fig. 1). As pointed out in Fig. 1, there are significant differences in the location of the C-terminus of $G\alpha_s$ between the model and the crystal structure. A distance of ~8 Å was observed between the C-termini of both models (Fig. 1).

Model I, which we predicted previously [12], is very similar to the crystal structure (3SN6) and reveals an RMSD of ~8.4 Å with regard to the corresponding parts of the crystal structure 3SN6 (Fig. 1). With regard to translation in the *x*-, *y*-, and *z*-directions, our predicted model I agrees very well with the crystal structure. Thus, in order to determine the set of angles $\alpha$, $\beta$, and $\gamma$ (Fig. 2a) that lead to the minimum RMSD between our predicted model and the crystal structure, we used model I as the starting structure and extended our potential surface scan in the following manner. Model I with $\alpha=\beta=\gamma=0°$ was used as the starting structure. $G\alpha_s$ was rotated systematically by $\alpha$, $\beta$, and $\gamma$ around the *x*-, *y*-, and *z*-axes (Fig. 2). The angles $\alpha$ and $\beta$ were varied in the range from −60° to 60° in steps of 15°, and $\gamma$ was varied in the range from −30° to 30° in steps of 15°. For each structure, energy minimization was performed using the same conditions and software as described previously [12]. Furthermore, the RMSDs between our structures and the corresponding parts of the crystal structure were calculated. The results are shown in Fig. 2b. This extended scan exhibited, that our predicted model I is the global minimum in the analyzed part of the potential energy surface (Fig. 2b, $\gamma=0°$, arrow a). Analysis of the RMSD surface shows a global minimum for $\alpha=45°$, $\beta=30°$, and $\gamma=15°$ (defined as model Ia) (Fig. 2b, $\gamma=15°$, arrow b). Here, the RMSD between the calculated complex and the corresponding parts of the crystal structure is ~3.3 Å. This RMSD is in the same range as that found when comparing $h\beta_2R$ structures (2.4 Å) and $G\alpha_s$ structures (3.5 Å), as mentioned above. Thus, this RMSD of 3.3 Å is mainly caused by the differences in the $h\beta_2R$ structures on the one hand and differences in the $G\alpha_s$ structures on the other, and only to a small degree by differences in the orientation of $h\beta_2R$ and $G\alpha_s$ with respect to each other. Based on these data, it can be stated that a rotation of $G\alpha_s$

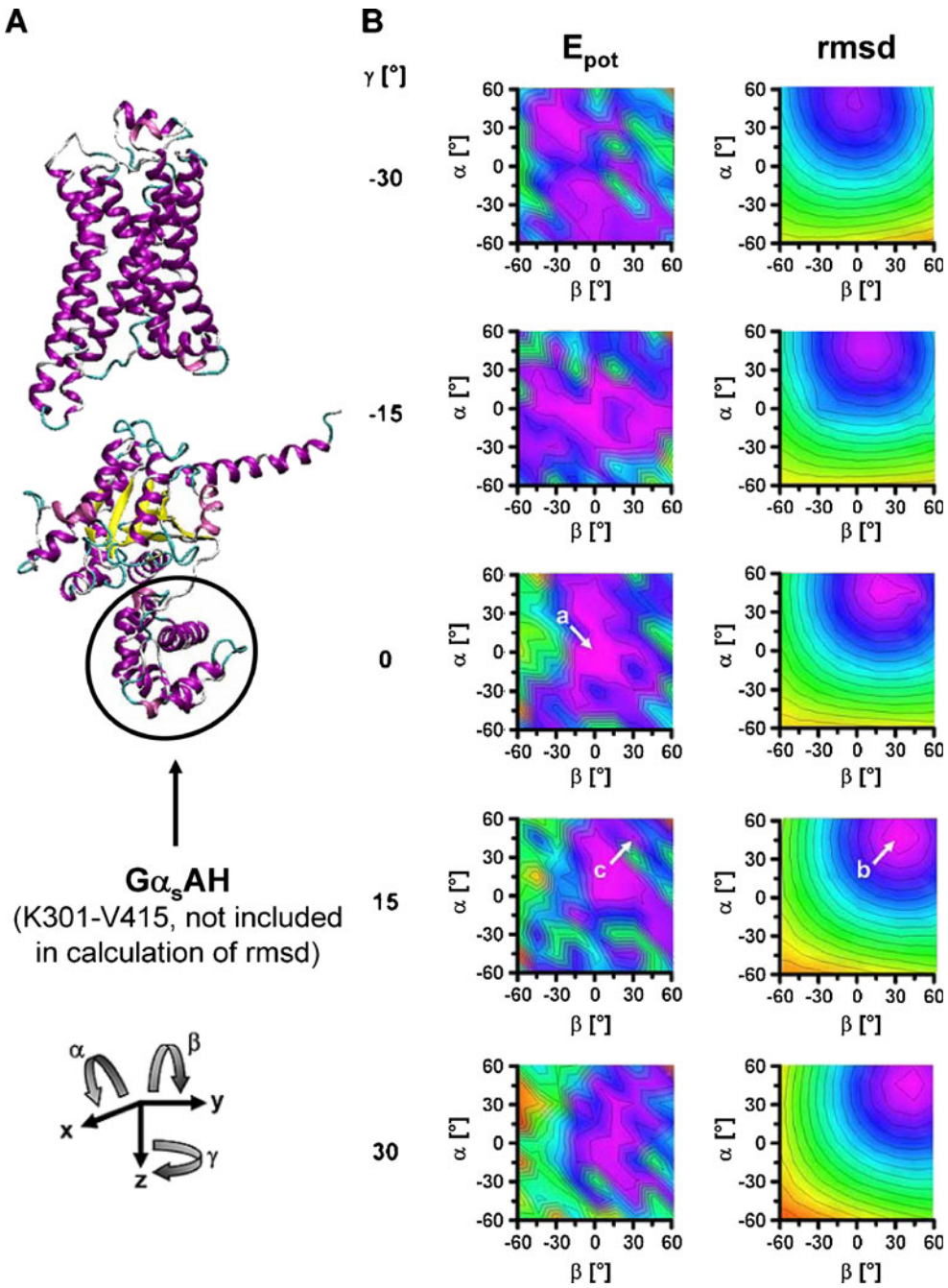


**Fig. 2** Modeling of the potential and RMSD surfaces of the $h\beta_2R$–$G\alpha_s$ complex. **a** Model of $h\beta_2R$ and $G\alpha_s$; the *black circle* indicates the $G\alpha_s$AH domain (K301–V415 [12]), which is not included in the alignment. **b** Potential energy ($E_{pot}$) and RMSD surfaces for the systematic search in the range $\alpha=\beta=-60$–$60°$, $\gamma=-30$–$30°$; *arrow a*: model I, representing a global minimum on the potential energy surface, as predicted previously [12]; *arrow b*: minimum RMSD between the calculated $h\beta_2R$–$G\alpha_s$ complex and the corresponding parts of the crystal structure; *arrow c*: local minimum on the potential energy surface, representing the smallest RMSD with regard to the crystal structure

in model I by $\alpha=45°$, $\beta=30°$, and $\gamma=15°$ (model Ia) results in an $h\beta_2R$–$G\alpha_s$ complex that is similar to the crystal structure 3SN6 (Fig. 3). Analysis of the potential energy shows that the energy of model Ia is about 15% higher than of model I. However, model Ia represents a local minimum on the potential energy surface (Fig. 2b, arrow C; Fig. 4a and b, point 1). Both minimum structures—model Ia (Fig. 4a and b, point 1) and model I (Fig. 4a and b, point 8)—can be connected by a minimum energy path by rotating $G\alpha_s$ by distinct angles $\alpha$, $\beta$, and $\gamma$ (Fig. 4a and b). A closer look at the contact surface between $h\beta_2R$ and $G\alpha_s$ in the minimum-RMSD model (model Ia) reveals two differences (Fig. 5). First, in the crystal structure 3SN6, there is greater outward movement of TM VI compared to our opsin-based homology model of $h\beta_2R$ (Fig. 5). Second, there are differences in the conformation of the helical C-terminus of $G\alpha_s$ between model Ia and the crystal structure (Fig. 5). These differences are caused by the template structures used for the homology modeling of $h\beta_2R$ and $G\alpha_s$. In general, analysis of the potential energy and the RMSD surface shows that model I [12] agrees very well with the experimentally determined crystal structure.

Aside from a surface scan, a subsequent molecular dynamics study of model Ia was performed in the same

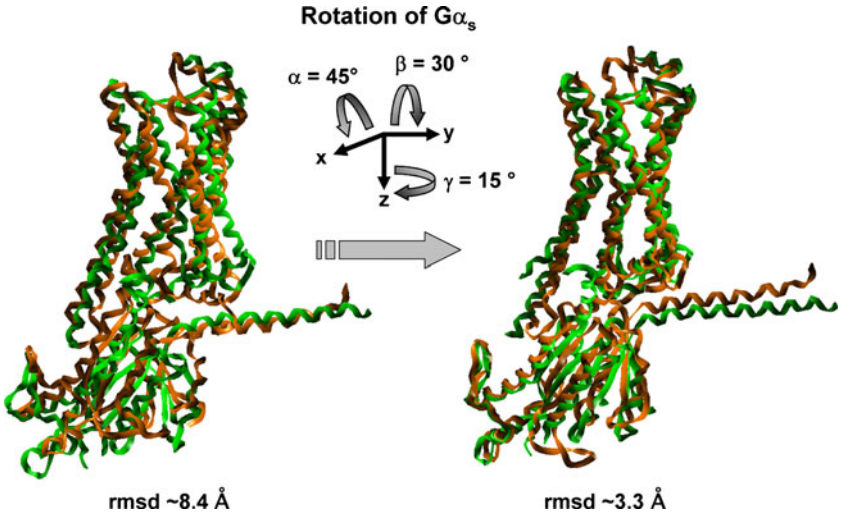


**Fig. 3** Alignment of model I or model Ia with the corresponding parts of the crystal structure 3SN6. The alignment of model I (*orange, left*) with the h$\beta_2$R–G$\alpha_s$ of the crystal structure (*green, left*) reveals an RMSD of ~8.4 Å, whereas the alignment of model Ia (*orange, right*) with the h$\beta_2$R–G$\alpha_s$ of the crystal structure (*green, right*) reveals a significantly smaller RMSD of ~3.3 Å. Rotating G$\alpha_s$ of model I by $\alpha$=45°, $\beta$=30°, and $\gamma$=15° results in model Ia

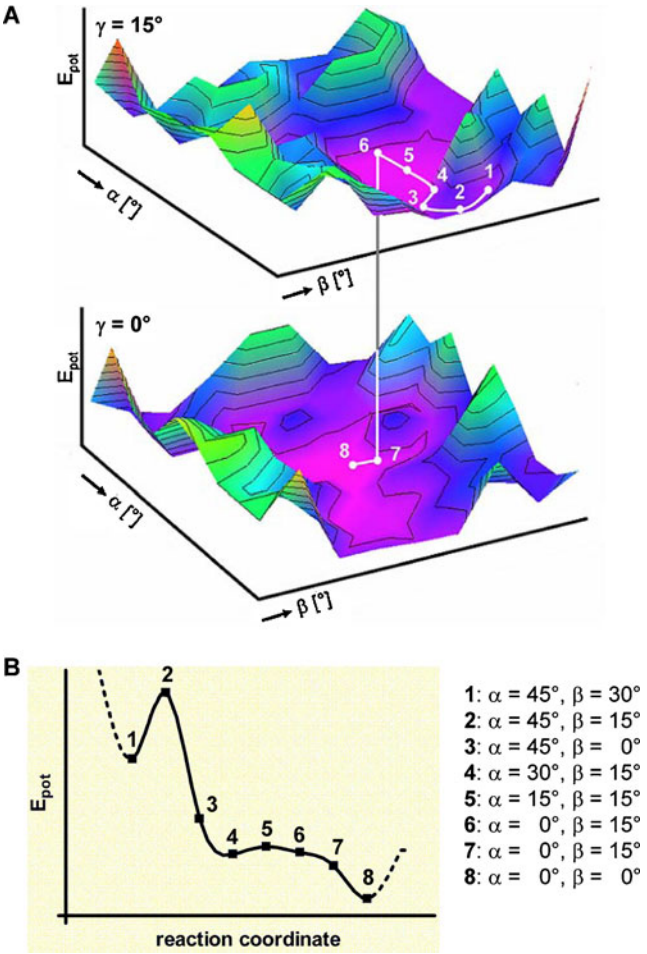


**Fig. 4** Potential energy surfaces of the predicted h$\beta_2$R–G$\alpha_s$ complex and the minimum-energy pathway. **a** Potential energy surface of the modeled h$\beta_2$R–G$\alpha_s$ complex for $\gamma$=15° and $\gamma$=0° along with the minimum-energy pathway connecting model Ia (*point 1*) and model I (*point 8*). Model I: $\alpha$=$\beta$=$\gamma$=0°. **b** Schematic presentation of the minimum energy pathway connecting model Ia (*point 1*) and model I (*point 8*) along with the corresponding angles $\alpha$, $\beta$, and $\gamma$

manner as in the corresponding previous study [12]. During the 2500 ps productive phase, the h$\beta_2$R–G$\alpha_s$ complex (model Ia) did not change significantly from the starting structure obtained using the surface scan. The simulations revealed a mean number of 12 hydrogen bonds between the h$\beta_2$R and G$\alpha_s$ (Fig. 6a). Fourteen pairs of hydrogen-bond interactions were observed (for >10% of the productive run) between h$\beta_2$R and G$\alpha_s$ (Fig. 6b). The interactions between 267K (h$\beta_2$R) and 419L (G$\alpha_s$) on the one hand and between 331D (h$\beta_2$R) and 417E (G$\alpha_s$) on the other were stable for >10% of the productive phase. Twelve pairs of hydrogen-bond interaction pairs between the h$\beta_2$R and G$\alpha_s$ were stable for more than 50% of the productive run, whereas six pairs were stable for more than 80% of the productive run (Fig. 6b). Model I also did not change significantly during the molecular dynamics study from the starting structure obtained using the surface scan [12]. Similar to model Ia, there were about eleven distinct hydrogen-bond interactions between the receptor and G$\alpha_s$ for more than 50% of the productive run in model I, and about six for more than 80% of the simulation [12]. This

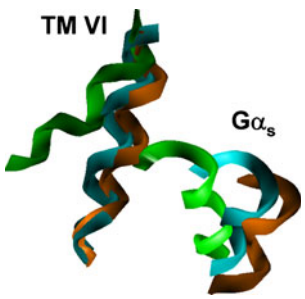


**Fig. 5** Alignment of h$\beta_2$R–G$\alpha_s$, opsin co-crystallized with part of the C-terminus of G$\alpha$, and model Ia. *Green* crystal structure of h$\beta_2$R–G$\alpha_s$ (3SN6), *cyan* crystal structure of opsin co-crystallized with part of the C-terminus of G$\alpha$ (3DQB), *orange* model Ia. Only the relevant parts of TM VI on the receptor and the C-terminus of G$\alpha$ are shown

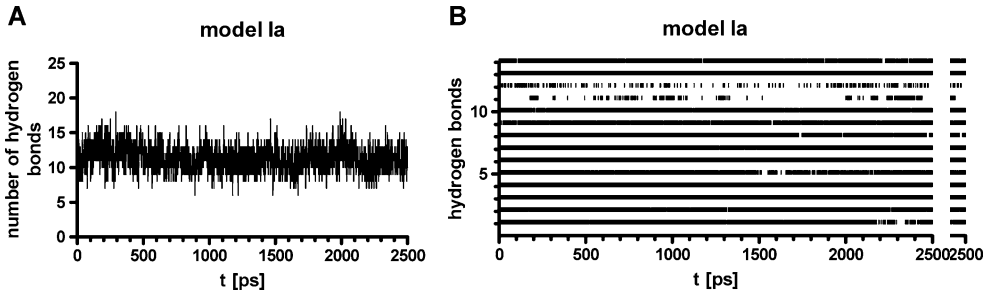


**Fig. 6** Hydrogen-bond interactions between $h\beta_2R$ and $G\alpha_s$ in model Ia. **a** Number of hydrogen bonds between $h\beta_2R$ and $G\alpha_s$ during the 2.5 ns productive phase in the MD simulation of the active $h\beta_2R$–$G\alpha_s$ complex of model Ia. **b** Distinct hydrogen-bond interactions (present for >10% of the productive run) between the active $h\beta_2R$–$G\alpha_s$ complex of model Ia: *1*, 131R–418L; *2*, 134A–413L; *3*, 135I–410R; *4*, 141Y–409Q; *5*, 225E–410R; *6*, 229Q–383Y; *7*, 229Q–385Y; *8*, 261A–374S; *9*, 263K–377S; *10*, 263K–381R; *11*, 267K–419L; *12*, 331D–417E; *13*, 332F–417E; *14*, 333R–417E

indicates that both models—model I and model Ia—are comparable not only in terms of stability but also with regards to the number of hydrogen-bond interactions between $h\beta_2R$ and $G\alpha_s$.

How valid are molecular modeling based predictions of GPCR–Gα complexes and of protein–protein complexes in general?

Before answering this question, the differences between both approaches (crystal structure on the one hand and molecular modeling on the other) need to be discussed. Crystal structures are snapshots of (for example) protein–protein complexes in the solid phase. However, in the cell, protein–protein complexes are located in a liquid phase, leading to flexibility in the surroundings and proteins. Thus, due to the different states (solid versus liquid), the most stable protein–protein conformation in the solid state is not necessarily the most stable conformation in the liquid phase. Indeed, differences are expected. In order to analyze the high number of structures (>650,000) generated during the surface scan within a reasonable computational time, only a very short computational time of about 0.5 min can be used for each point on the surface. This is achieved by performing "only" energy minimizations. However, in this case, neither the surroundings nor the flexibility of the complex are taken into account. To compensate for this approximation, distinct complex conformations can be embedded into the surroundings and MD simulations can be performed. Unfortunately, since MD simulations are highly time-consuming, a complete MD scan of all $h\beta_2R$–$G\alpha_s$ complexes cannot be performed. Therefore, in our predictive study [12], only two distinct minimum structures were analyzed by MD simulations. To perform MD simulations on a significantly higher number of complexes with low potential energies, a large number of CPUs is needed in general.

Also, it is important to be aware that, in order to facilitate the crystallization of the $h\beta_2R$–$G\alpha\beta\gamma$ complex, two additional proteins had to be introduced: the Gs-binding nanobody (Nb35), which binds between the Gα and Gβ subunits [14], and T4 lysozyme, which is fused to the amino terminus of $h\beta_2R$ [14]. Since neither of these proteins are native to the $h\beta_2R$–$G\alpha\beta\gamma$ complex, distinct influences of the Nb35 nanobody and T4 lysozyme on the crystal structure must be taken into account; especially with regard to Nb35, which is localized between Gα and Gβ [14]. This can cause differences in the contact area and conformations of $h\beta_2R$ and $G\alpha_s$ for example.

Mutagenesis studies were performed in order to determine interaction sites between the biogenic amine receptor and the corresponding Gα subunit [15]. However, not all of the experimental results can be explained using one model [16]. Thus, a hypothesis involving sequential binding of Gα to the receptor has been discussed [17]. Based on all of the experimental results (crystal structures and the energy surface scan), this hypothesis of sequential binding can be supported. It is suggested that both minima (represented by model I and model Ia) are involved in the sequential binding process. As already mentioned, crystal structures are snapshots of distinct conformations in the solid state, but in molecular modeling studies, these local minima can be connected by minimum-energy pathways.

Mutagenesis studies, when combined with appropriate pharmacological experiments, can provide hints about the amino acids that are involved in the receptor–Gα interaction. However, detailed information about distinct interaction sites between the receptor and Gα at the molecular level cannot be obtained by such experiments. Also, while crystal structures are—as already mentioned above—artificial, information based on crystal structures or other experimental studies can simplify the surface scan, because they can provide some idea of where both proteins may interact with each other, which enables the systematic surface scan to be focused on defined areas. This is very important from the perspective of achieving reasonable computational times. In contrast, molecular modeling studies afford insight into distinct

amino acid interactions between the receptor and Gα, and intermediate states (complexes that are not represented by a minimum on the energy surface) can be calculated. Thus, modeling data can hint at the interaction sites between $h\beta_2R$ and $G\alpha_s$, and so they provide a platform for useful experimental studies: well-directed mutagenesis and pharmacological assays. However, more experimental data are needed in combination with molecular modeling studies in order to prove the hypothesis of a sequential binding mechanism.

Summarizing, it is clear that reasonable results can be obtained from predictive molecular modeling studies of GPCR–Gα complexes. However, additional experimental studies must be performed in order to obtain the complete and correct picture of the GPCR–Gα interaction at the molecular level, and to verify the predictions obtained from molecular modeling. It should be noted that obtaining crystal structures of GPCR–Gαβγ complexes is not a standard technique. In contrast, molecular modeling studies represent a fast technique for predicting interactions between GPCR and Gα. It can thus be concluded that molecular modeling studies are, when used in combination with experimental studies, a valuable tool for predicting protein–protein complexes.

## References


1. Kristiansen K (2004) Molecular mechanisms of ligand binding, signaling, and regulation within the superfamily of G-protein-coupled receptors: molecular modeling and mutagenesis approaches to receptor structure and function. Pharmacol Ther 103:21–80
2. Oldham WM, Hamm HE (2006) Structural basis of function in heterotrimeric G proteins. Q Rev Biophys 39:117–166
3. Pierce KL, Premont RT, Lefkowitz RJ (2002) Seven-transmembrane receptors. Nat Rev Mol Cell Biol 9:639–650
4. Gether U, Kobilka BK (1998) G Protein-coupled receptors. II. Mechanism of agonist activation. J Biol Chem 273:17979–17982
5. Wall MA, Coleman DE, Lee E, Iniguez-Lluhi JA, Posner BA, Gilman AG, Sprang SR (1995) The structure of the G protein heterotrimer Gi alpha 1 beta 1 gamma 2. Cell (Cambridge, MA) 83:1047–1058
6. Cherezov V, Rosenbaum DM, Hanson MA, Rasmussen SGF, Thian FS, Kobilka TS, Choi HJ, Kuhn P, Weis WI, Kobilka BK, Stevens RC (2007) High-resolution crystal structure of an engineered human $\beta_2$-adrenergic G protein-coupled receptor. Science 318:1258–1265
7. Rasmussen SGF, Choi HJ, Rosenbaum DM, Kobilka TS, Thian FS, Edwards PC, Burghammer M, Ratnala VRP, Sanishvili R, Fischetti RF, Schertler GFX, Weis WI, Kobilka BK (2007) Crystal structure of the human $\beta_2$ adrenergic G-protein-coupled receptor. Nature 450:383–387
8. Rosenbaum DM, Cherezov V, Hanson MA, Rasmussen SGF, Thian FS, Kobilka TS, Choi HJ, Yao XJ, Weis WI, Stevens RC, Kobilka BK (2007) GPCR engineering yields high-resolution structural insights into $\beta_2$-adrenergic receptor function. Science 318:1266–1273
9. Warne T, Serrano-Vega MJ, Baker JG, Moukhametzianov R, Edwards PC, Henderson R, Leslie AG, Tate CG, Schertler GF (2008) Structure of a $\beta_1$-adrenergic G protein-coupled receptor. Nature 454:486–491
10. Jaakola VP, Griffith MT, Hanson MA, Cherezov V, Chien YET, Lane JR, Ijzerman AP, Stevens RC (2008) The 2.6 Å crystal structure of a human $A_{2A}$ adenosine receptor bound to an antagonist. Science 322:1211–1217
11. Scheerer P, Park JH, Hildebrand PW, Kim YJ, Krauß N, Choe HW, Hofmann KP, Ernst OP (2008) Crystal structure of opsin in its G-protein-interacting conformation. Nature 455:497–503
12. Straßer A, Wittmann HJ (2010) Distinct interactions between the human adrenergic $\beta_2$ receptor and $G\alpha_s$: an in silico study. J Mol Model 16:1307–1318
13. Sunahara RK, Tesmer JJ, Gilman AG, Sprang SR (1997) Crystal structure of the adenylyl cyclase activator Gsα. Science 278:1943–1947
14. Rasmussen SGF, DeVree BT, Zou Y, Kruse AC, Chung KY, Kobilka TS, Thian FS, Chae PS, Pardon E, Calinski D, Mathiesen JM, Shah STY, Lyons JA, Caffrey M, Gellman SH, Steyaert J, Skiniotis G, Weis WI, Sunahara RK, Kobilka BK (2011) Crystal structure of the $\beta_2$ adrenergic receptor–Gs protein complex. Nature. doi:10.1038/nature10361
15. Grishina G, Bertlot CH (2000) A surface-exposed region of $G_s\alpha$ in which substitutions decrease receptor-mediated activation and increase receptor affinity. Mol Pharmacol 57:1081–1092
16. Oldham WM, Hamm HE (2008) Heterotrimeric G protein activation by G-protein-coupled receptors. Nat Rev Mol Cell Biol 9:60–71
17. Herrmann R, Heck M, Henklein P, Henklein P, Kleuss C, Hofmann KP, Ernst OP (2004) Sequence of interactions in receptor–G protein coupling. J Biol Chem 279:24283–24290